Electronic Supplementary Material (ESI) for Journal of Materials Chemistry A.

The Hierarchical Nanowires Array of Iron Phosphide Integrated on Carbon Fiber Paper as an Effective Electrocatalyst for Hydrogen Generation

Cuncai Lv,[a] Zhen Peng, [b] Yaoxing Zhao, [a] Zhipeng Huang,[*a] and Chi Zhang [*a]

[a] *Functional Molecular Materials Research Centre, Scientific Research Academy, Jiangsu University, Zhenjiang 212013, P. R. China.*

[b] *School of Materials Science and Engineering, Jiangsu University, Zhenjiang 212013, P. R. China.*

* Corresponding author: Zhipeng Huang, Chi Zhang;

E-mail: zphuang@ujs.edu.cn; chizhang@ujs.edu.cn; Phone/Fax: +86-511-88797815

Electronic Supplementary Information

Synthesis 1: Synthesis of CFP-CoP NA

In this experiment, cobalt chloride carbonate hydroxide ($Co(CO_3)_{0.35}Cl_{0.20}(OH)_{1.10}$) nanowires array was grown on CFP by hydrothermal reaction at 120 °C in a 50 mL Teflon-lined stainless-steel autoclave with a piece of cleaned CFP (2 cm x 5 cm) and 40 mL aqueous solution containing $CoCl_2•6H_2O$ (0.952 g) and $CO(NH_2)_2$ (0.240 g) for 6 hours. Afterwards, the CFP-$Co(CO_3)_{0.35}Cl_{0.20}(OH)_{1.10}$ nanowires array was converted to CFP-CoP nanowires array (CFP-CoP NA) by phosphidation using NaH_2PO_2 (0.8 g) as phosphorus source in 350 °C tube furnace for 1 hour in N_2 flow.

Synthesis 2: Synthesis of CFP-FeP NA

In this experiment, iron oxide hydroxide (FeO(OH)) nanorods array was grown on CFP by hydrothermal reaction at 120 °C in a 50 mL Teflon-lined stainless-steel autoclave with a piece of cleaned CFP (2 cm x 5 cm) and 40 mL aqueous solution containing $FeCl_3•6H_2O$ (0.457 g) and Na_2SO_4 (0.274 g) for 6 hours. To prepare the CFP-FeP nanorods array (CFP-FeP NA), the CFP-FeO(OH) nanorods array was annealed at 350 °C for 1 hour in tube furnace in N_2 flow using NaH_2PO_2 (0.8 g) as phosphorus source.

Synthesis 3: Synthesis of FeP nanorods powder and CFP/FeP nanorods

In this experiment, the powder of iron oxide hydroxide (FeO(OH)) nanorods was prepared by hydrothermal reaction at 120 °C in a 50 mL Teflon-lined stainless-steel autoclave with 40 mL aqueous solution containing $FeCl_3 \bullet 6H_2O$ (0.457 g) and Na_2SO_4 (0.274 g) for 6 hours. The brown product was isolated and washed by repeated centrifugation/ultrasonication with deionized water. Finally, the product was dried under vacuum at 60 °C. To prepare the powder of FeP nanorods, the FeO(OH) nanorods was annealed at 350 °C for 1 hour in tube furnace in N_2 flow using NaH_2PO_2 (0.8 g) as phosphorus source.

To prepare the CFP/FeP nanorods, FeP nanorods (10 mg) and Nafion solution (5 wt%, 80 μL) were dispersed in 1 ml of water/ethanol (4/1, v/v) by ultrasonication (ultrasonic probe, 2 mm diameter, 130 W, 1 h) to form homogeneous ink. The dispersion (34 μL) was dropped onto a piece of cleaned CFP, which were sealed with tape with the exception of an exposed area 0.3 cm × 0.3 cm) and dried naturally. The CFP was cleaned by sonication sequentially in acetone, water and ethanol for 10 min each prior to the drop casting of the FeP nanorods.

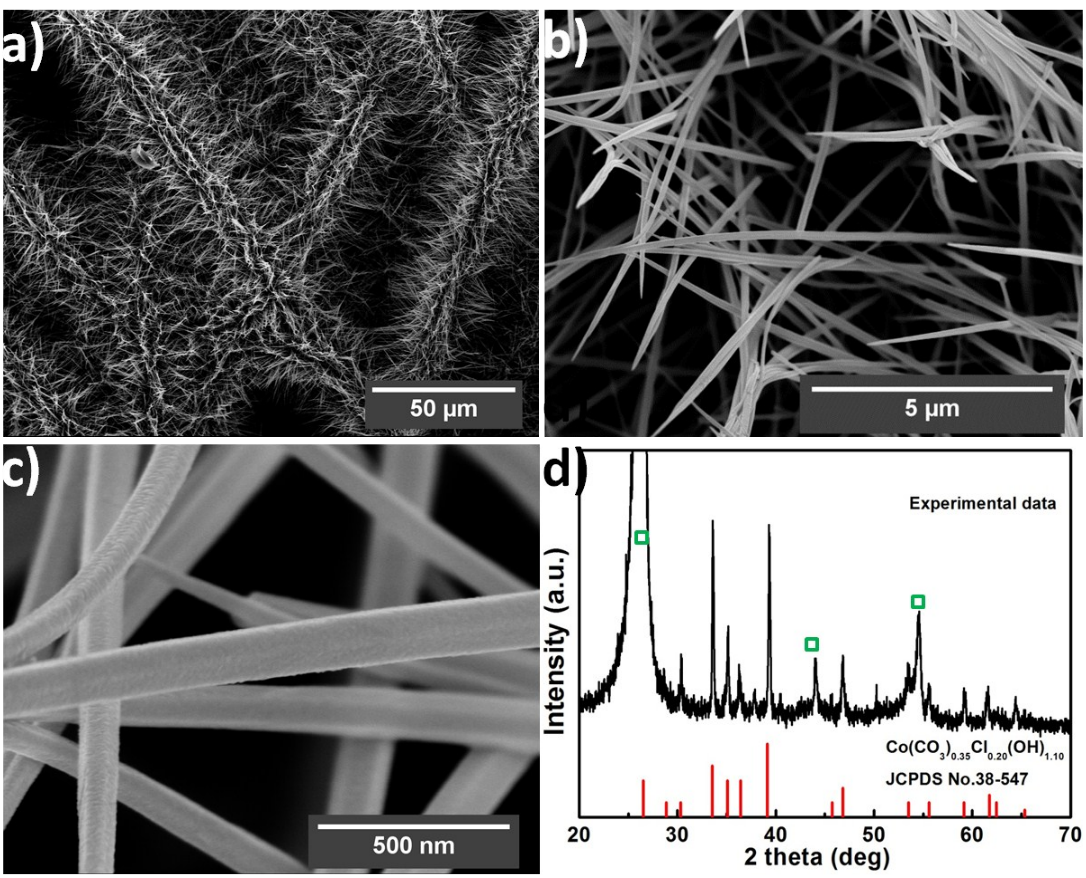

Figure S1. (a, b) Low- and (c) high-magnification SEM images, (d) XRD pattern of CFP-$Co(CO_3)_{0.35}Cl_{0.20}(OH)_{1.10}$ NA (In the panel d, the peaks of CFP are marked by □) .

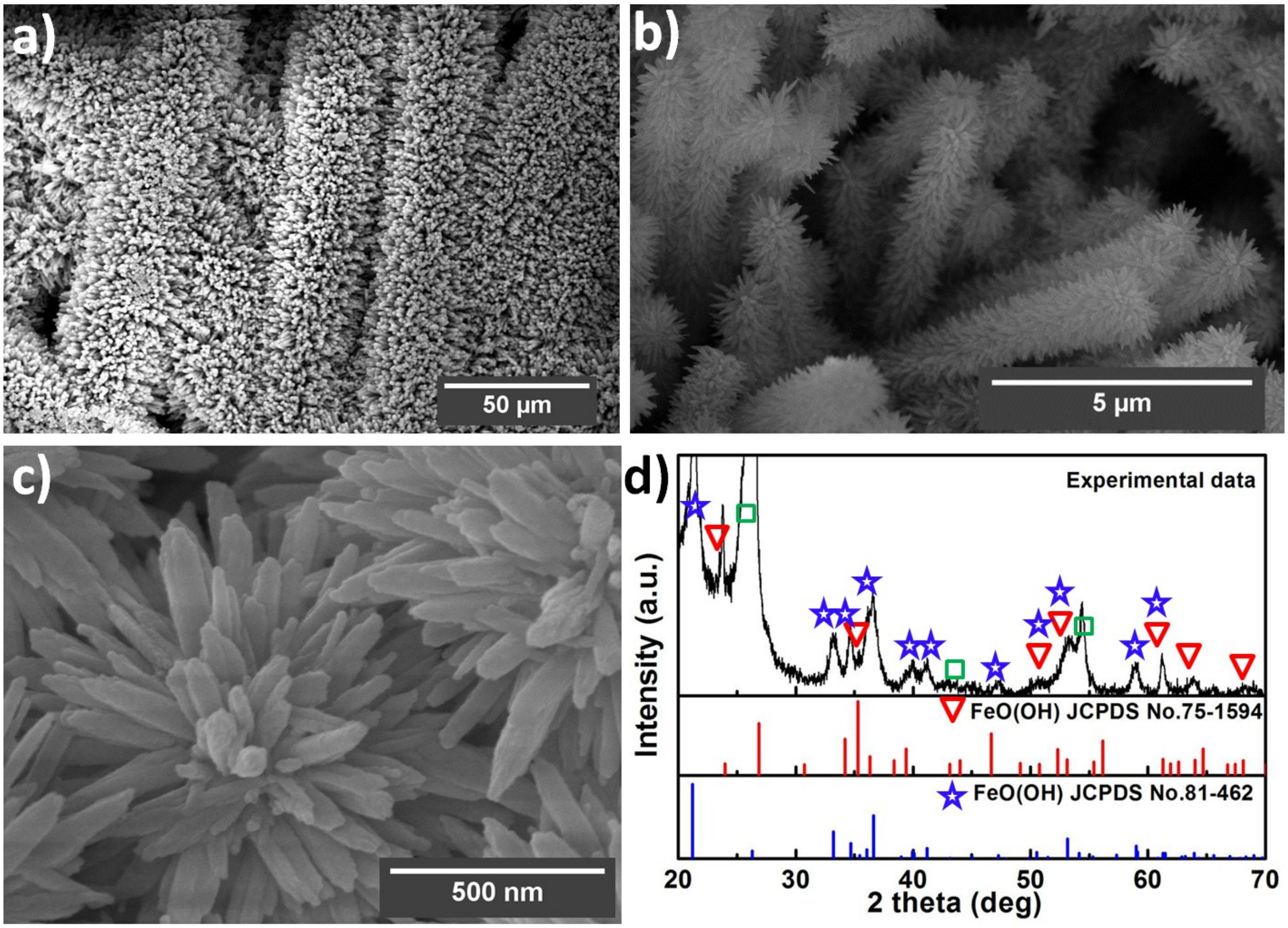

Figure S2. (a, b) Low- and (c) high-magnification SEM images, (d) XRD pattern of CFP- FeO(OH) HNA. (In the panel d, the peaks of CFP are marked by □.)

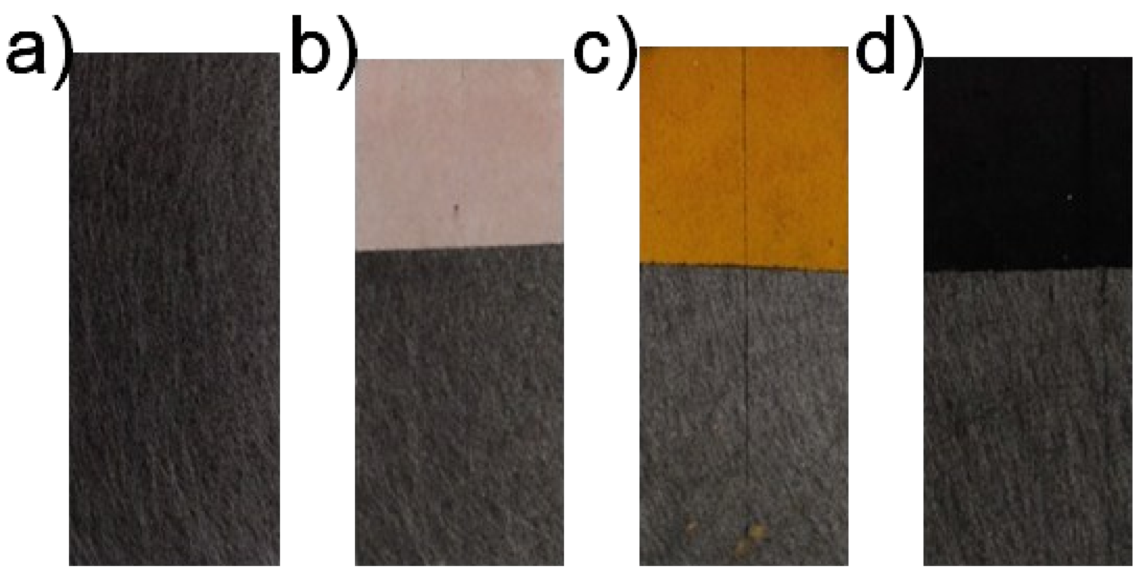

Figure S3. Optical photograph of the (a) Pristine CFP, (b) CFP-$Co(CO_3)_{0.35}Cl_{0.20}(OH)_{1.10}$ NA, (c) CFP-FeO(OH) HNA, (d) CFP- FeP HNA

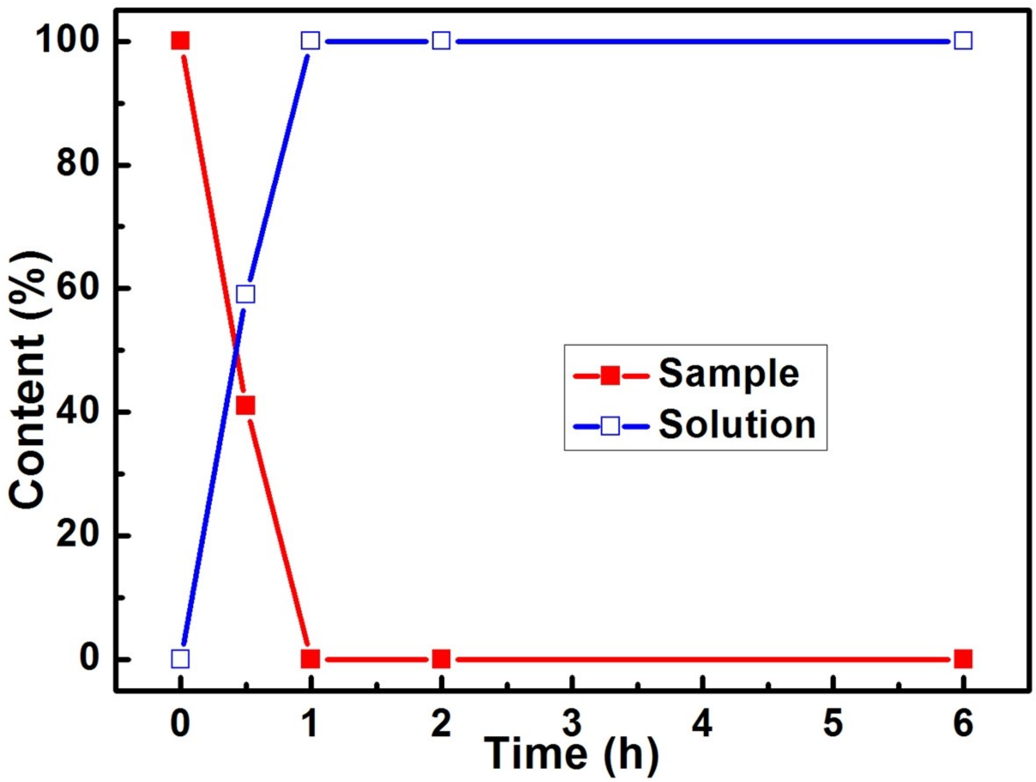

Figure S4. The ratio of the amount of cobalt in the CFP-FeO(OH) HNA to that in the solution after the hydrothermal growth of CFP-FeO(OH) HNA.

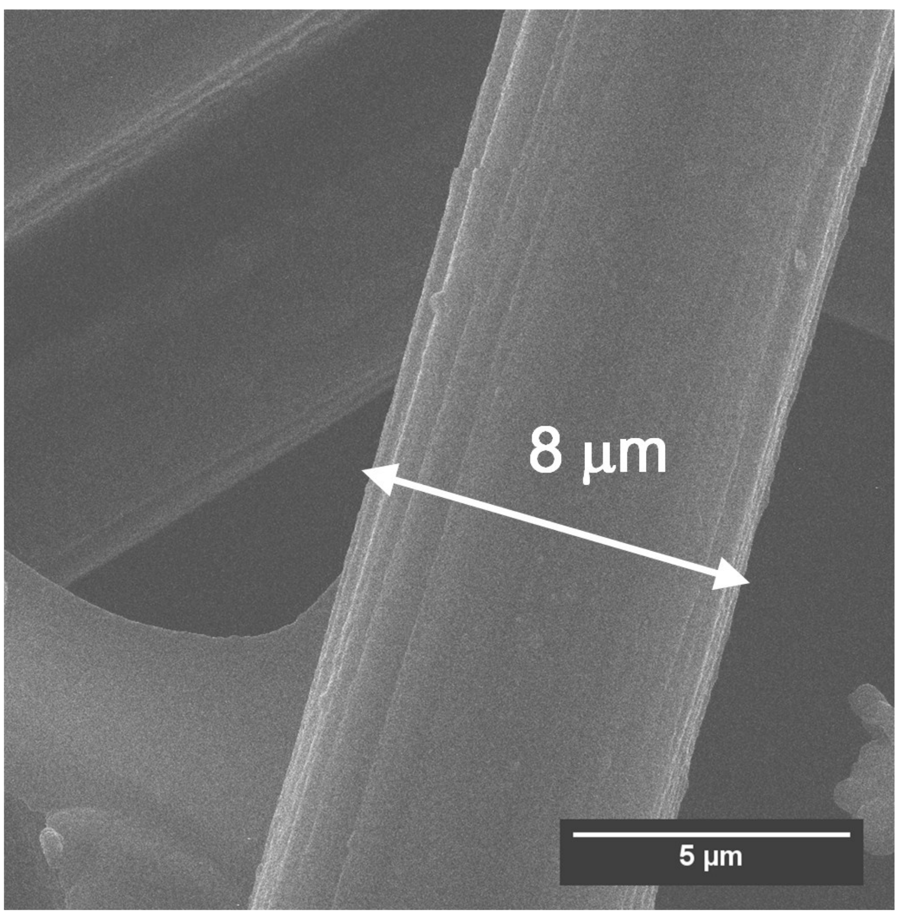

Figure S5. SEM image of the pristine CFP.

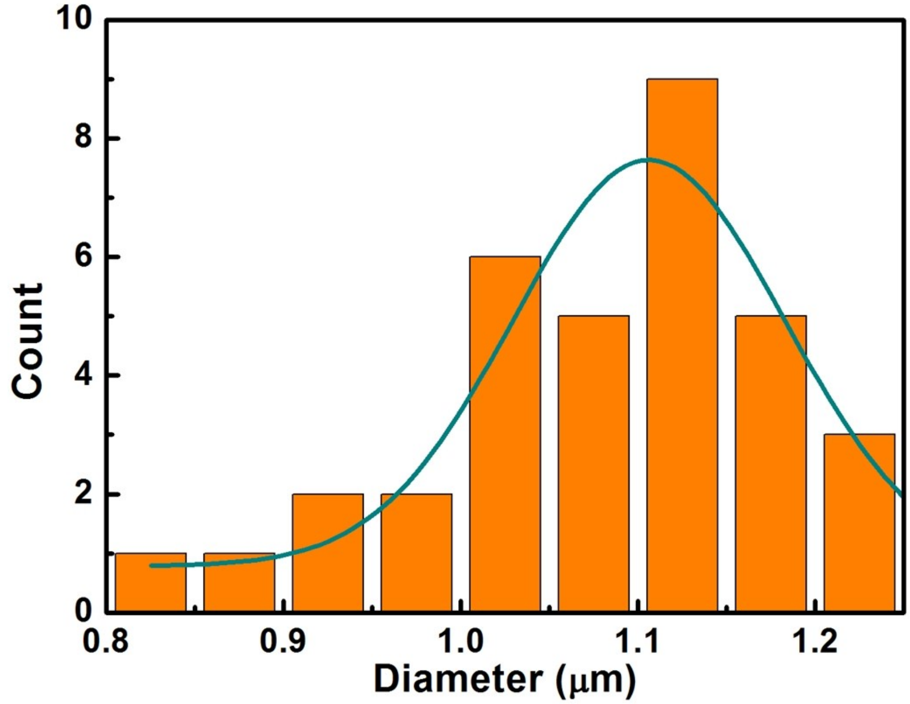

Figure S6. Diameter distribution of FeP HNA. The dark cyan line shows the Gaussian fitting of data.

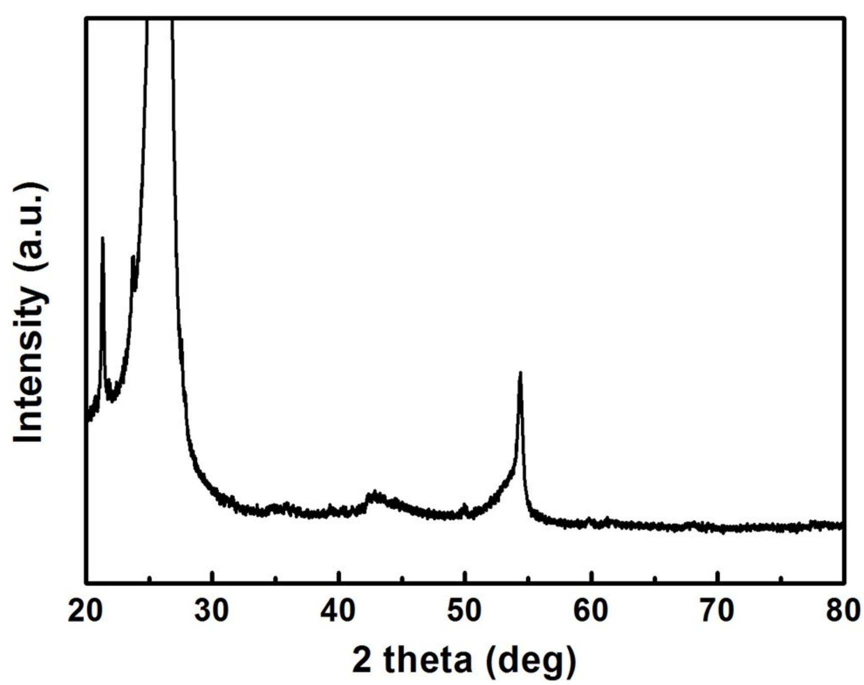

Figure S7. XRD pattern of pristine CFP

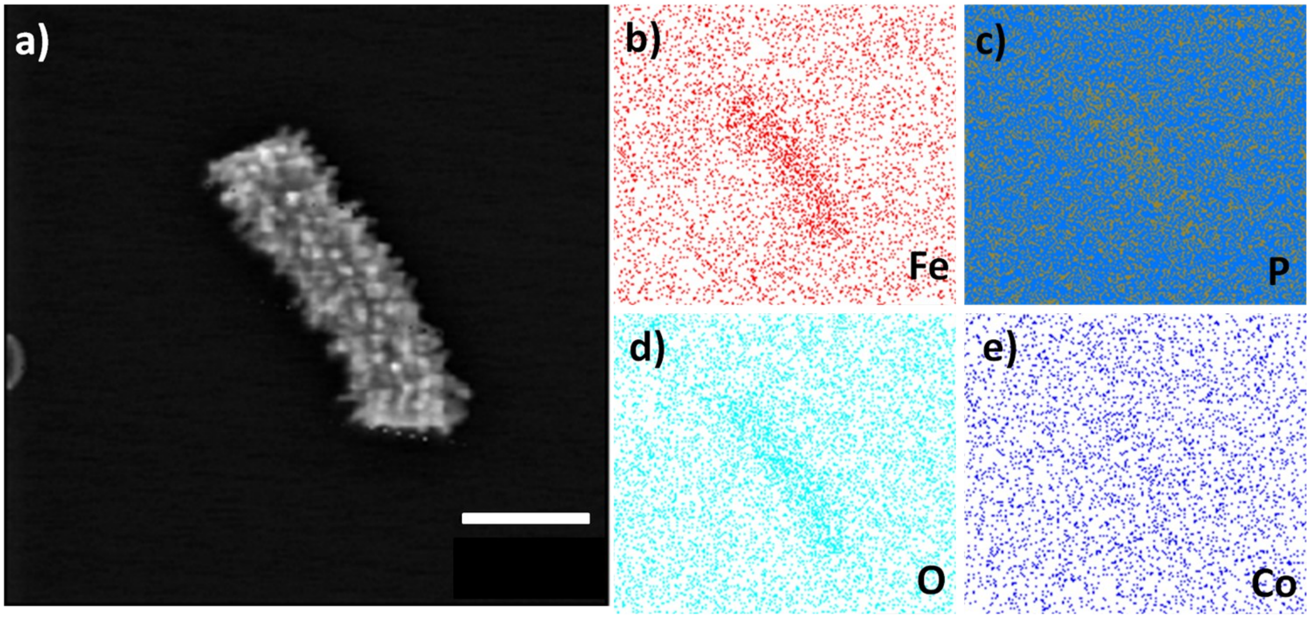

Figure S8. (a) SEM image recorded by a high-angle annular dark-field detector. The scale bar in (a) is 2 μm. Elemental maps for the spatial distribution of (b) Fe, (c) P, (d) O and (e) Co obtained from the EDX elemental mapping of region indicated by the square in (a).

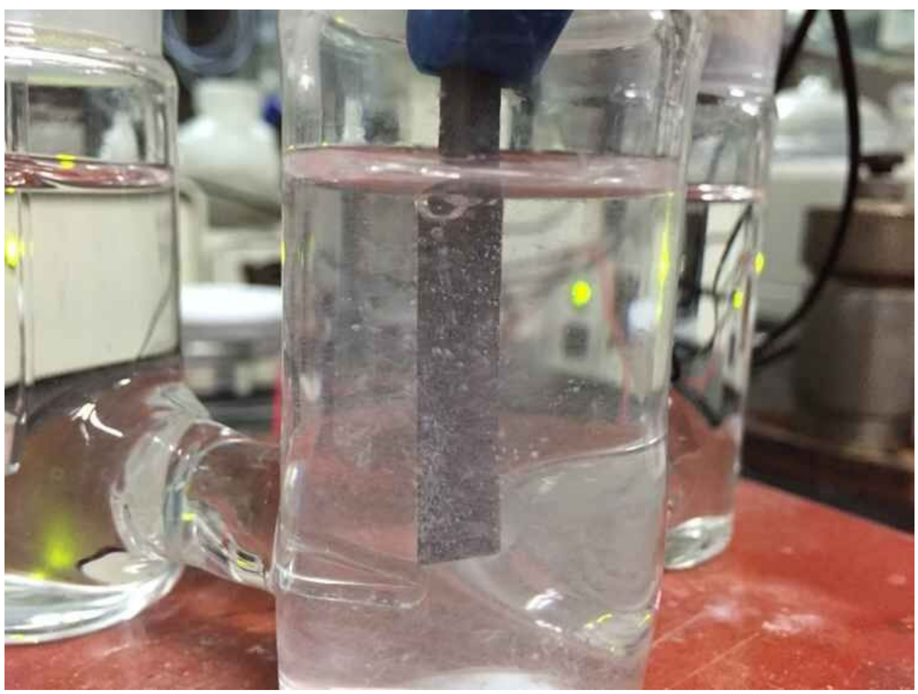

Figure S9. Optical photograph of the CFP-FeP HNA during the measurement.

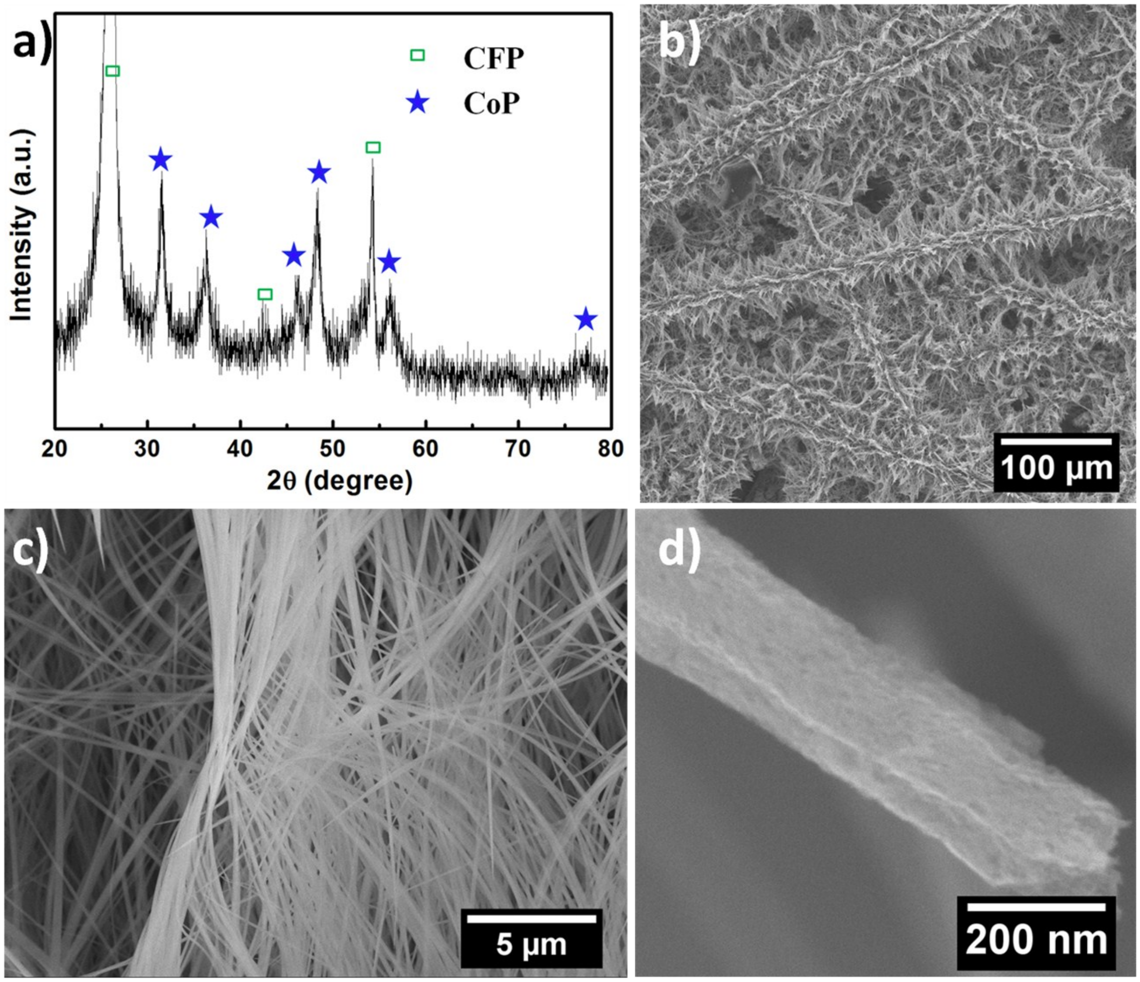

Figure S10. (a) XRD pattern, (b, c) Low- and (d) high-magnification SEM images of CFP-CoP NA.

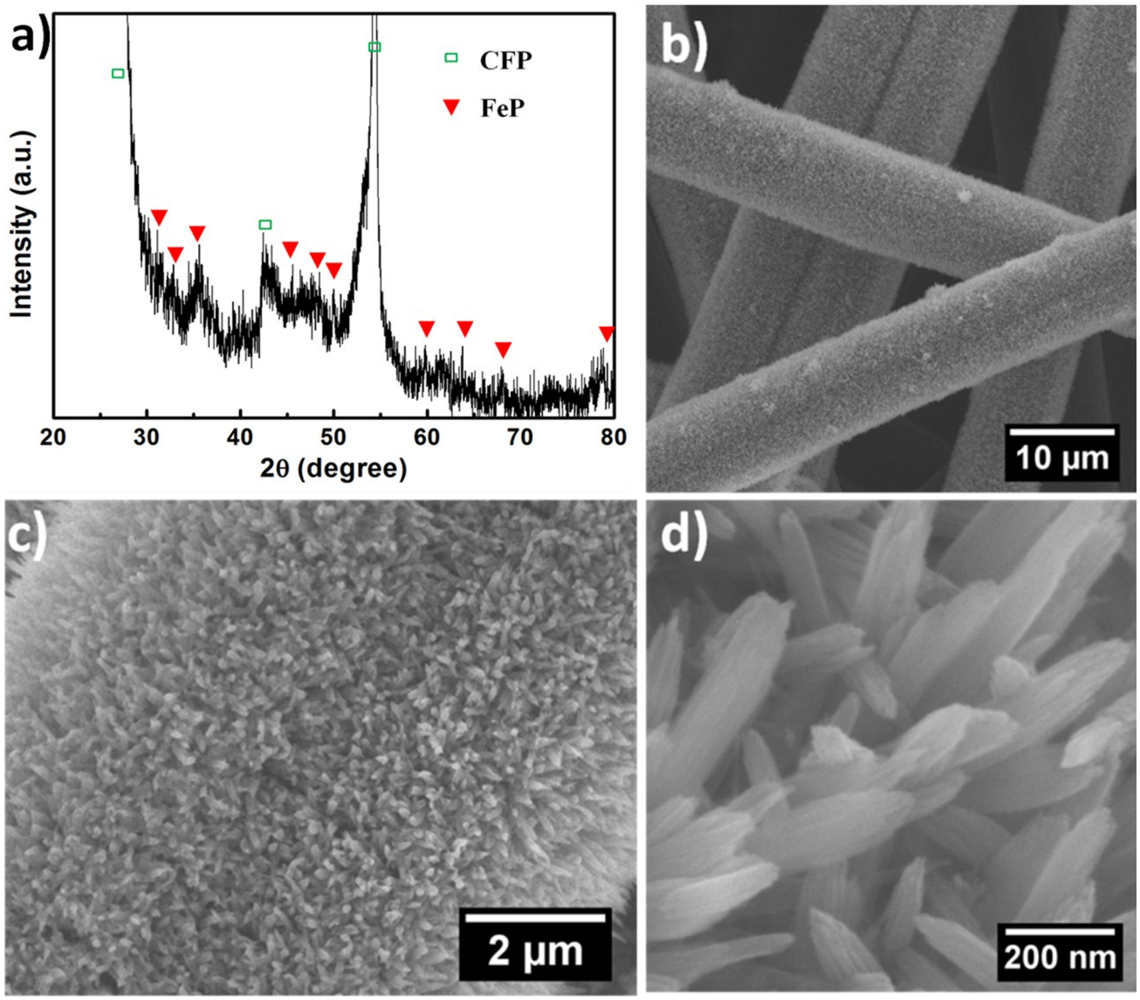

Figure S11. (a) XRD pattern, (b, c) Low- and (d) high-magnification SEM images of CFP-FeP NA.

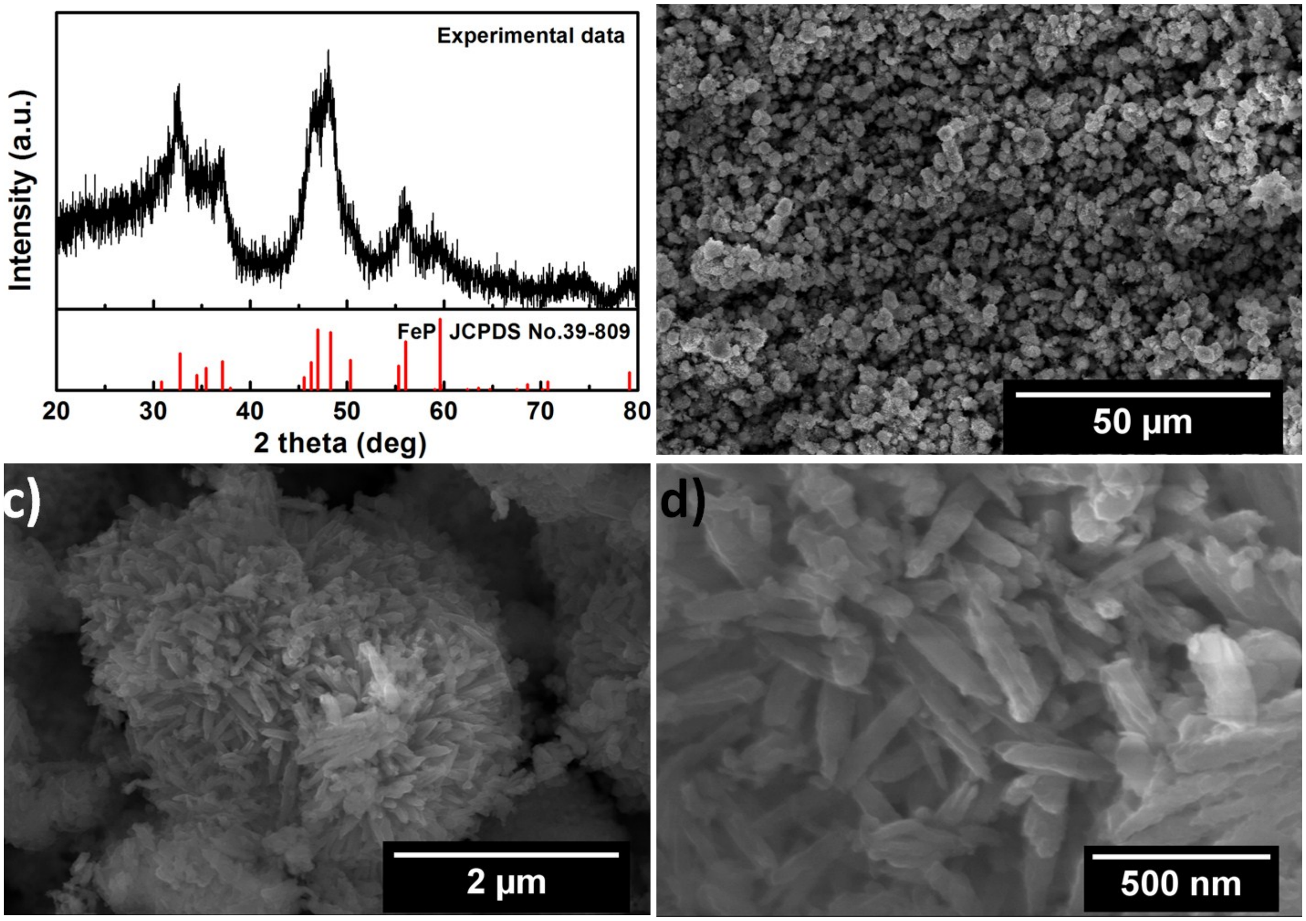

Figure S12. (a) XRD pattern, (b, c) Low- and (d) high-magnification SEM images of FeP nanorods.

Table S1. Summary of HER performance of representative catalysts.

Catalyst	Substrate	Mass density (mg/cm^2)	η_{10} (mV)	η_{20} (mV)	Tafel slope (mV/dec)	J_0 (mA/cm^2)	Electrolyte
Ni_2P nanoparticle[1]	Ti foil	1	117	130	$46_{\eta=25-125}$ $81_{\eta=150-200}$	3.3×10^{-2}	0.50M H_2SO_4
Ni_2P nanoparticle[2]	GCE	0.38		140	87		0.50M H_2SO_4
$Ni_{12}P_5$ nanoparticle[3]	GCE	3		141			0.50M H_2SO_4
NiP_2nanosheet on carbon cloth[4]	Carbon cloth	4.3		99	51	0.26	0.50M H_2SO_4
CoP nanoparticle[5]	Ti foil	0.9		95	50	1.4×10^{-1}	0.50M H_2SO_4
CoPnanorod on carbon cloth[6]	carbon cloth	0.92		100	51	2.8×10^{-1}	0.50M H_2SO_4
CoP particle on carbon nanotube[7]	GCE	0.285	122		54	1.3×10^{-1}	0.50M H_2SO_4

Co_2P nanorod[8]	GCE	1		167			0.50M H_2SO_4
FeP nanoparticles[9]	Ti foil	1	50	61	37	4.3×10^{-1}	0.50M H_2SO_4
FePnanorods[10]	Ti foil	3.2		72	38	4.2×10^{-1}	0.50M H_2SO_4
Porous FePnanosheet[11]	GCE			325	67		
MoP nanoparticle [12]	GCE	0.36	125		54	8.6×10^{-2}	0.50M H_2SO_4
MoP nanoparticle[13]	GCE			160	54	3.4×10^{-2}	0.50M H_2SO_4
Cu_3P nanowires on copper foam[14]	copper foam	15.7	143		67	1.8×10^{-1}	0.50M H_2SO_4
Ni-Mo nanopowder[15]	Ti foil	1		70			2 M NaOH
Ni-Mo nanopowder[15]	Ti foil	3		80			0.5 M H_2SO_4
Ni-Mo nanopowder[15]	Ti foil	1	79	107			1 M NaOH
Bulk Mo_2C[16]	carbon paste electrode	1.4	208	224	$56_{\eta=100-220}$	1.3×10^{-3}	0.50 M H_2SO_4
Bulk MoB[16]	carbon paste electrode	2.5	212	227	$55_{\eta=140-210}$	1.4×10^{-3}	0.50 M H_2SO_4
Mo_2C/CNT[17]	carbon paper	2	149		55.2	1.4×10^{-2}	0.1 M $HClO_4$
Fe-WCN [18]	RRDE	0.4	220		47.1		H_2SO_4(pH 1) + Na_2SO_4 (0.5 M)
Mo_1Soy[19]	carbon paper	1.4	177		66.4	1.3×10^{-2}	0.1 M $HClO_4$
Mo_2C[20]	GCE	0.357	200	210-220	55.8-64.5		0.50M H_2SO_4
Porous Mo_2C nanowire[21]	GCE	0.21		150	53		0.50M H_2SO_4
Mo_2C on Gr[22]	GCE	0.285		~160	54		0.50M H_2SO_4
MoWC nanowire[23]	GCE	1.28		~160	56	3.4×10^{-3}	0.50M H_2SO_4
Mo_1Soy-RGO[19]	carbon paper	0.47	109		62.7	3.7×10^{-2}	0.1 M $HClO_4$

Mo_2C/C[19]	carbon paper	2	311		87.6	8.1×10^{-3}	0.1 M $HClO_4$
$Co_{0.6}Mo_{1.4}N_2$[24]	GCE	0.243	202	267		2.3×10^{-4}	0.1M $HClO_4$
MoS_3(33%)/MWCNT-NC[25]	silver electrode	0.255	206	226	$40_{\eta=135-174}$	1.35×10^{-4}	1 M H_2SO_4
Core-shell MoO_3-MoS_2nanowires[26]	FTO		254	272	$50-60_{\eta=200}$		0.5 M H_2SO_4
Defect-rich MoS_2nanosheets[27]	GCE	0.285	190	214	$50_{\eta=120-180}$	8.91×10^{-3}	0.5 M H_2SO_4
MoS_2@Au[28]	Au electrode	0.00103	226		69	9.3×10^{-3}	0.5 M H_2SO_4
amorphous MoS_3-CV[29]	GCE		211	229	$40_{\eta=170-200}$	1.3×10^{-4}	1 M H_2SO_4
MoS_2/RGO hierarchical[30]	GCE	0.285	154	176	41		0.5M H_2SO_4
MoS_2/MGF[31]	GCE	0.21	146	159	$42_{\eta=90-120}$		0.5 M H_2SO_4
MoS_2/CNTs[32]	glass carbon disk	0.136	184	230	44.6		0.5 M H_2SO_4
Cu_2MoS_4[33]	GCE	0.0425	321		95		pH0 H_2SO_4
WS_2/RGO[34]	GCE	0.4	265	292	58		0.5M H_2SO_4
WS_2nanosheets[35]	GCE	0.0001-0.0002or ca. one continuous layer	233	275	55		0.5 M H_2SO_4
WS_2nanosheets[36]	GCE	0.285	151	177	72	2.5×10^{-3}	1 M H_2SO_4
Cobalt-sulfide catalyst[37]	FTO		165	227	93		1.0 M pH 7 PBS
$NiWS_x$[38]	FTO		373	430	$96_{\eta=120-150}$	$10^{-2.66}$	pH 7 PBS
$CoWS_x$[38]	FTO		271	311	$78_{\eta=120-150}$	$10^{-2.25}$	pH 7 PBS
$CoMoS_x$[38]	FTO		241	282	$85_{\eta=120-150}$	$10^{-2.89}$	pH 7 PBS
FeS_2[39]	GCE		192.6		62.5	7×10^{-4}	0.5 M H_2SO_4
$FeSe_2$[39]	GCE				65.3	3.5×10^{-4}	0.5 M H_2SO_4
$Fe_{0.43}Co_{0.57}S_2$[39]	GCE		264		55.9	1.3×10^{-3}	0.5 M H_2SO_4
CoS_2[39]	GCE		232		44.6	6.5×10^{-5}	0.5 M H_2SO_4
$CoSe_2$[39]	GCE	0.037	231		42.4	6.5×10^{-5}	0.5 M H_2SO_4
$Co_{0.56}Ni_{0.44}Se_2$[39]	GCE		250		49.7	6.3×10^{-5}	0.5 M

							H_2SO_4
$Co_{0.32}Ni_{0.68}S_2$[39]	GCE				66.8	3.0×10^{-4}	0.5 M H_2SO_4
NiS_2[39]	GCE				41.6	1.4×10^{-4}	0.5 M H_2SO_4
$NiSe_2$[39]	GCE		250		56.9	5.7×10^{-4}	0.5 M H_2SO_4
Ni_5P_4/Ni foil[40]	Ni foil	100	140		40		0.5 M H_2SO_4
FeP/CC[41]	Carbon Cloth		34	43	29.2		0.5 M H_2SO_4

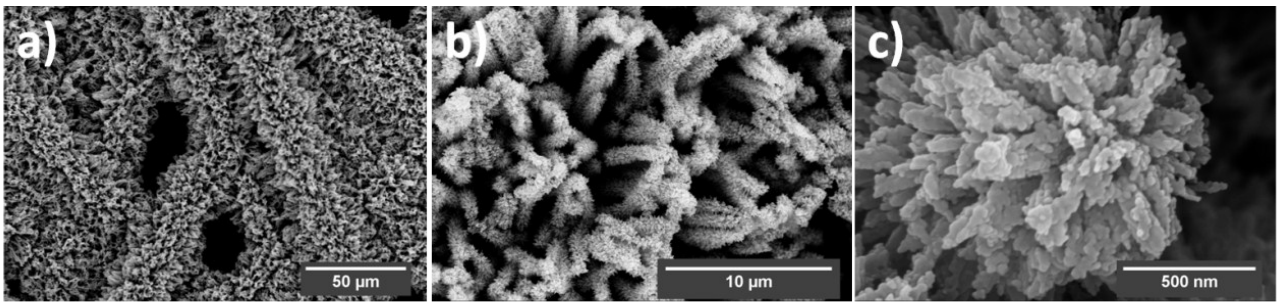

Figure S13. (a, b) Low- and (c) high-magnification SEM images of CFP- FeP HNA after the electrochemical measurement.

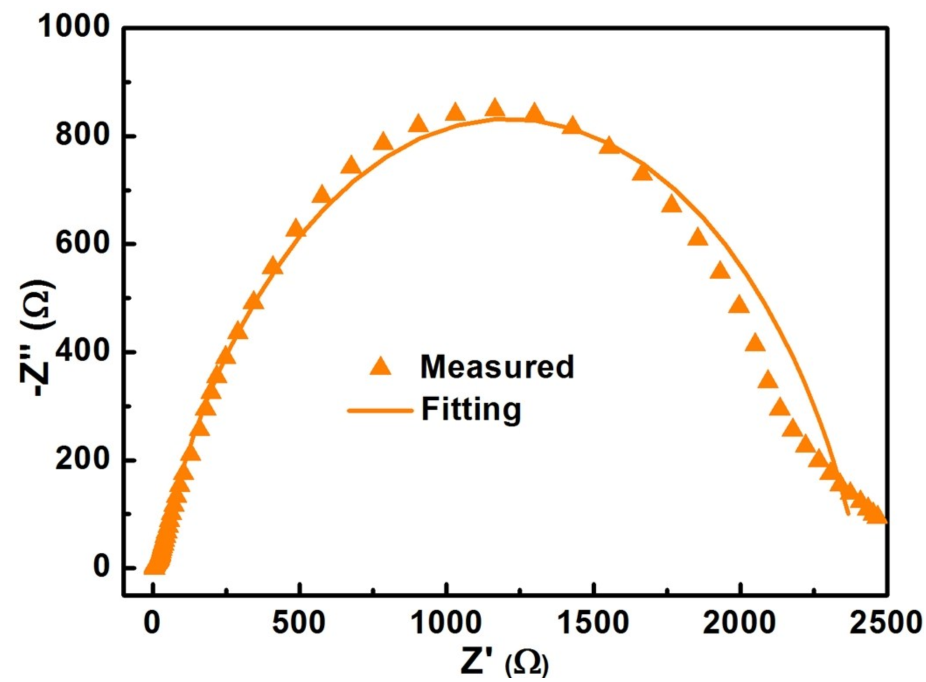

Figure S14. Nyquist plots of EIS spectra measured of CFP/FeP nanorods.

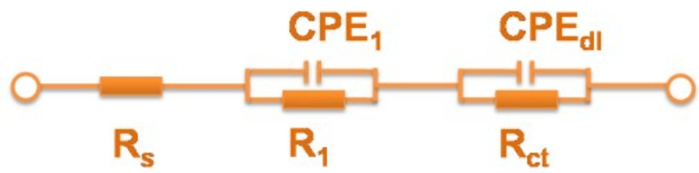

Figure S15. Equivalent circuit used to fit the EIS data. R_s is the overall series resistance, CPE_1 and R_1 are the constant phase element and resistance describing electron transport at substrate/catalyst interface, respectively, CPE_{dl} is the constant phase element of the catalyst/electrolyte interface, and R_{ct} is the charge transfer resistance at catalyst/electrolyte interface.

Table S2. The fitting results of EIS spectra

Sample	R_s (Ω)	Q_{ct} (F cm^{-2} S^{n-1})	N_{ct}	R_{ct} (Ω)	Q_1 (F cm^{-2} S^{n-1})	n_1	R_1 (Ω)
CFP- FeP HNA	1.909	5.802e-6	0.7708	12.05	0.04222	0.7398	11.01
CFP-CoP NA	1.816	9.502e-3	0.7458	29.95	1.5e-5	0.6844	11.84
CFP- FeP NA	2.139	1.768e-5	0.6919	64.86	3.427e-3	0.8063	10.18
CFP/FeP nanorods	5.191	1.658e-4	0.7738	2392	8.61e-6	1	12.09

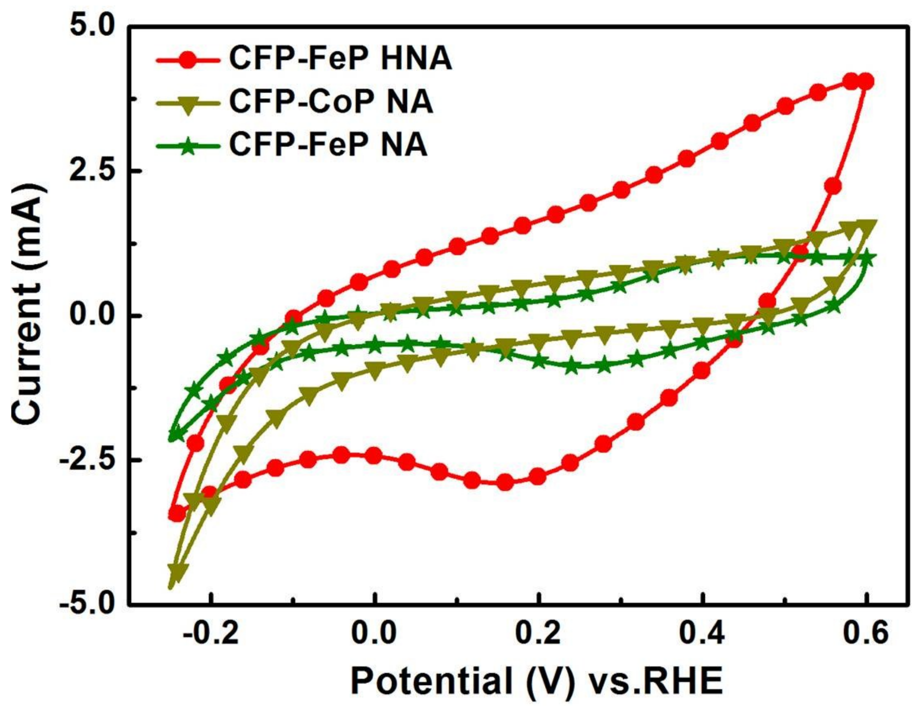

Figure S16. The CVs in the region of −0.2 to 0.6 V vs RHE for CFP- FeP HNA, CFP-CoP NA, and CFP-FeP NA at pH 7 (scan rate: 50 mV s^{-1}).

References

1. E. J. Popczun, J. R. McKone, C. G. Read, A. J. Biacchi, A. M. Wiltrout, N. S. Lewis and R. E. Schaak, *J. Am. Chem. Soc.*, 2013, **135**, 9267-9270.
2. L. G. Feng, H. Vrubel, M. Bensimon and X. L. Hu, *Phys. Chem. Chem. Phys.*, 2014, **16**, 5917-5921.
3. Z. P. Huang, Z. B. Chen, Z. Z. Chen, C. C. Lv, H. Meng and C. Zhang, *Acs Nano*, 2014, **8**, 8121-8129.
4. M. Gong, W. Zhou, M. Tsai, J. Zhou, M. Guan, M. Lin, B. Zhang, Y. Hu, D. Wang, J. Yang, S. J. Pennycook, B.-J. Hwang and D. Hongjie, *Nat. Commun.*, 2014, **5**, 4695.
5. E. J. Popczun, C. G. Read, C. W. Roske, N. S. Lewis and R. E. Schaak, *Angew. Chem. Int. Ed.*, 2014, **53**, 5427-5430.
6. J. Q. Tian, Q. Liu, A. M. Asiri and X. P. Sun, *J. Am. Chem. Soc.*, 2014, **136**, 7587-7590.
7. Q. Liu, J. Q. Tian, W. Cui, P. Jiang, N. Y. Cheng, A. M. Asiri and X. P. Sun, *Angew. Chem. Int. Ed.*, 2014, **53**, 6710-6714.
8. Z. P. Huang, Z. Z. Chen, Z. B. Chen, C. C. Lv, M. G. Humphrey and C. Zhang, *Nano Energy*, 2014, **9**, 373-382.
9. J. F. Callejas, J. M. McEnaney, C. G. Read, J. C. Crompton, A. J. Biacchi, E. J. Popczun, T. R. Gordon, N. S. Lewis and R. E. Schaak, *ACS Nano*, 2014, **8**, 11101-11107.
10. P. Jiang, Q. Liu, Y. H. Liang, J. Q. Tian, A. M. Asiri and X. P. Sun, *Angew. Chem. Int. Ed.*, 2014, **53**, 12855-12859.
11. Y. Xu, R. Wu, J. F. Zhang, Y. M. Shi and B. Zhang, *Chem. Commun.*, 2013, **49**, 3.
12. Z. C. Xing, Q. Liu, A. M. Asiri and X. P. Sun, *Adv. Mater.*, 2014, **26**, 5702-5707.
13. P. Xiao, M. A. Sk, L. Thia, X. M. Ge, R. J. Lim, J. Y. Wang, K. H. Lim and X. Wang, *Energ. Environ. Sci.*, 2014, **7**, 2624-2629.
14. J. Q. Tian, Q. Liu, N. Y. Cheng, A. M. Asiri and X. P. Sun, *Angew. Chem. Int. Ed.*, 2014, **53**, 9577-9581.
15. J. R. McKone, B. F. Sadtler, C. A. Werlang, N. S. Lewis and H. B. Gray, *ACS Catal.*, 2013, **3**, 166-169.
16. H. Vrubel and X. L. Hu, *Angew. Chem. Int. Ed.*, 2012, **51**, 12703-12706.
17. W. F. Chen, C. H. Wang, K. Sasaki, N. Marinkovic, W. Xu, J. T. Muckerman, Y. Zhu and R. R. Adzic, *Energ. Environ. Sci.*, 2013, **6**, 943-951.
18. Y. Zhao, K. Kamiya, K. Hashimoto and S. Nakanishi, *Angew. Chem. Int. Ed.*, 2013, **52**, 1-5.
19. W. F. Chen, S. Iyer, S. Iyer, K. Sasaki, C. H. Wang, Y. M. Zhu, J. T. Muckerman and E. Fujita, *Energ. Environ. Sci.*, 2013, **6**, 1818-1826.
20. C. J. Ge, P. Jiang, W. Cui, Z. H. Pu, Z. C. Xing, A. M. Asiri, A. Y. Obaid, X. P. Sun and J. Tian, *Electrochim. Acta*, 2014, **134**, 182-186.
21. L. Liao, S. N. Wang, J. J. Xiao, X. J. Bian, Y. H. Zhang, M. D. Scanlon, X. L. Hu, Y. Tang, B. H. Liu and H. H. Girault, *Energ. Environ. Sci*, 2014, **7**, 387-392.
22. L. F. Pan, Y. H. Li, S. Yang, P. F. Liu, M. Q. Yu and H. G. Yang, *Chem. commun.*, 2014, **50**, 13135-13137.
23. P. Xiao, X. M. Ge, H. B. Wang, Z. L. Liu, A. Fisher and X. Wang, *Adv. Funct. Mater.*, 2015, **25**, 1520-1526.
24. B. F. Cao, C. M. Veith, J. C. Neuefeind, R. R. Adzic and P. G. Khalifah, *J. Am. Chem. Soc.*, 2013, **135**, 19186-19192.

25. T. W. Lin, C. J. Liu and J. Y. Lin, *Appl. Catal. B- Environ.*, 2013, **134-135**, 75-82.
26. Z. Chen, D. Cummins, B. N. Reinecke, E. Clark, M. K. Sunkara and T. F. Jaramillo, *Nano Lett.*, 2011, **11**, 4168-4175.
27. J. Xie, H. Zhang, S. Li, R. Wang, X. Sun, M. Zhou, J. Zhou, X. W. Lou and Y. Xie, *Adv. Mater.*, 2013, **25**, 5807-5813.
28. T. Y. Wang, L. Liu, Z. W. Zhu, P. Papakonstantinou, J. B. Hu and M. Li, *Energ. Environ. Sci.*, 2013, **6**, 625-633.
29. D. Merki, S. Fierro, H. Vrubel and X. L. Hu, *Chem. Sci.*, 2011, **2**, 1262-1267.
30. Y. Li, H. Wang, L. Xie, Y. Liang, G. Hong and H. Dai, *J. Am. Chem. Soc.*, 2011, **133**, 7296-7299.
31. L. Liao, J. Zhu, X. J. Bian, L. N. Zhu, M. D. Scanlon, H. H. Girault and B. H. Liu, *Adv. Funct. Mater.*, 2013, **23**, 5326-5333.
32. Y. Yan, X. Ge, Z. Liu, J. Y. Wang, J. M. Lee and X. Wang, *Nanoscale*, 2013, **5**, 7768-7771.
33. P. D. Tran, M. Nguyen, S. S. Pramana, A. Bhattacharjee, S. Y. Chiam, J. Fize, M. J. Field, V. Artero, L. H. Wong, J. Loo and J. Barber, *Energ. Environ. Sci.*, 2012, **5**, 8912-8916.
34. J. Yang, D. Voiry, S. J. Ahn, D. Kang, A. Y. Kim, M. Chhowalla and H. S. Shin, *Angew. Chem. Int. Ed.*, 2013, **52**, 13751-13754.
35. D. Voiry, H. Yamaguchi, J. Li, R. Silva, D. C. Alves, T. Fujita, M. Chen, T. Asefa, V. B. Shenoy, G. Eda and M. Chhowalla, *Nat. Mater.*, 2013, **12**, 850-855.
36. Z. Z. Wu, B. Z. Fang, B. Arman, A. K. Sun, D. P. Wilkinson and D. Z. Wang, *Appl. Catal. B-Environ.*, 2012, **125**, 59-66.
37. Y. Sun, C. Liu, D. C. Grauer, J. Yano, J. R. Long, P. Yang and C. J. Chang, *J. Am. Chem. Soc.*, 2013, **135**, 17699-17702.
38. P. D. Tran, S. Y. Chiam, P. P. Boix, Y. Ren, S. S. Pramana, J. Fize, V. Artero and J. Barber, *Energ. Environ. Sci.*, 2013, **6**, 2452-2459.
39. D. S. Kong, J. J. Cha, H. T. Wang, H. R. Lee and Y. Cui, *Energ. Environ. Sci.*, 2013, **6**, 3553-3558.
40 M. Ledendecker, S. K. Calderón, C. Papp, H. P. Steinrück, M. Antonietti, M. Shalom, *Angew. Chem. Int. Ed.*, 2015, **54**, 1-6
41 X. Yang, A. Y. Lu, Y. Zhu, S. Min, M. N. Hedhili, Y. Han, K. W. Huang, L. J. Li, *Nanoscale*, 2015,**7** , 10974-10981